

Bioinformatics Combined With Experimental Modeling to Study the Molecular Mechanism of Xuefu Zhuyu Decoction to Improve Erectile Dysfunction Associated With Asthma in Rats

American Journal of Men's Health
November-December 1–18
© The Author(s) 2024
Article reuse guidelines:
sagepub.com/journals-permissions
DOI: 10.1177/15579883241293936
journals.sagepub.com/home/jmh


Junlong Feng^{1,2*} , Sheng Deng^{3*}, Xuefeng Gong^{4*}, Bin Wang¹, Longji Sun¹, Huanan Zhang¹, Zixiang Gao^{1,2}, Hui Chen^{1,2}, Kali Zou⁵, Jiaqi Yang^{1,2}, Haisong Li¹, and Jisheng Wang¹ 

Abstract

Asthma is associated with chronic systemic inflammation, and inflammatory factors can damage vascular endothelial cells, thus impairing erectile function (ED). Xuefu Zhuyu decoction (XFZYD) can inhibit inflammation and promote angiogenesis, which in turn improves asthma as well as ED, but its exact mechanism of action is not yet clear. This study investigates the mechanism underlying the beneficial effect of XFZYD on asthma-associated ED. High-performance liquid chromatography-tandem mass spectrometry (HPLC-MS/MS) was used to analyze the constituents of XFZYD, and network pharmacology analysis was used to predict the target genes of XFZYD. Sprague–Dawley rats in the asthma model with erectile dysfunction were divided into the model, XFZYD low-, medium-, and high-dose group (3.09, 6.17, and 12.34 g/kg), with drug intervention for 8 weeks. We assessed the interleukin 6 (IL-6), vascular endothelial growth factor A (VEGFA), and tumor necrosis factor (TNF) protein levels in the penile tissue. We discovered that after treatment with XFZYD (3.09, 6.17, and 12.34 g/kg), the number of erections significantly increased (1.17 ± 0.41 , 1.50 ± 0.55 , and 1.67 ± 0.52), the density of endothelial cells in the corpus cavernosum of the penis increased, the expression level of IL-6 was reduced (7.5%, 21.2%, and 24.4%), the expression level of VEGFA was reduced (7.8%, 25%, and 28.4%), and the expression level of TNF was reduced (13.5%, 30.6%, and 32.4%). The in vivo experiments indicate that XFZYD may improve ED in asthma model rats by inhibiting inflammation and reducing vascular permeability. This study provides new insights into the mechanism of action of XFZYD in the treatment of asthma leading to ED.

Keywords

classical formula, network pharmacology, target, erectile dysfunction

Received August 15, 2024; revised September 29, 2024; accepted October 3, 2024

¹Department of Andrology, Dongzhimen Hospital, Beijing University of Chinese Medicine, Beijing, China

²Beijing University of Chinese Medicine, Beijing, China

³Department of Andrology, Shunyi Hospital of Beijing Traditional Chinese Medicine Hospital, Beijing, China

⁴Department of Traditional Chinese Medicine, Beijing Chaoyang Hospital, Beijing, China

⁵Department of Emergency, Dongzhimen Hospital, Beijing University of Chinese Medicine, Beijing, China

*Junlong Feng, Sheng Deng, and Xuefeng Gong contributed equally to this work and share first authorship.

Corresponding Authors:

Haisong Li, Department of Andrology, Dongzhimen Hospital, Beijing University of Chinese Medicine, Beijing 100700, China.

Email: lihs396@sina.com

Jisheng Wang, Department of Andrology, Dongzhimen Hospital, Beijing University of Chinese Medicine, Beijing 100700, China.

Email: houdejisheng@sina.com



Creative Commons Non Commercial CC BY-NC: This article is distributed under the terms of the Creative Commons Attribution-NonCommercial 4.0 License (<https://creativecommons.org/licenses/by-nc/4.0/>) which permits non-commercial use, reproduction and distribution of the work without further permission provided the original work is attributed as specified on the SAGE and Open Access pages (<https://us.sagepub.com/en-us/nam/open-access-at-sage>).

Introduction

Asthma is a common condition characterized by chronic airway inflammation, which includes restricted airflow and wheezing, dyspnea, chest tightness, cough, and other symptoms (Papi et al., 2018). Asthma affects approximately 334 million people worldwide, and severe cases are associated with diminished quality of life (QoL), disability, and increased mortality risk (Vos et al., 2012). Asthma is associated with chronic systemic inflammation; in this condition, inflammatory agents can harm vascular endothelial cells, which compromise erectile function (Chou et al., 2011). In men, erectile dysfunction (ED) is a common type of sexual dysfunction that can negatively affect interpersonal relationships and QoL (Burnett et al., 2018).

Patients with asthma are more likely to have ED than patients without asthma. It has been demonstrated that the severity of ED has positively correlated with the severity of asthma (C. C. Lu, 2012). According to studies, asthma can increase inflammatory factors such as interleukin 6 (IL-6) and tumor necrosis factor (TNF), and the protein vascular endothelial growth factor A (VEGFA), which can then damage cavernous vascular endothelial cells and impair erectile function. In addition, it can increase vascular permeability and aggravate the inflammatory response (J. S. Wang et al., 2020). In addition, studies have shown that asthma can cause a decrease in endothelial nitric oxide synthase (eNOS) levels and eNOS activity, leading to a decrease in nitric oxide (NO) levels and cyclic guanosine monophosphate (cGMP) concentrations in cavernous tissues, resulting in ED in rats (Zou et al., 2015).

The first-line treatment for ED is phosphodiesterase-5 inhibitors (PDE5is), which frequently produce positive clinical results (L. Chen et al., 2015). Asthmatic patients presenting with ED do not respond well to PDE5is (Grigoryan et al., 2018), and oral PDE5 does not raise circulating GMP levels to the threshold necessary for erection, even when asthmatics maintain normal breathing (Dorsey et al., 2010; Vinay et al., 2021). But at the same time, there is evidence that Chinese medicine can provide safe and effective treatments for ED. Chinese medicine plays an increasingly important role in the treatment of many diseases and disorders (J. S. Wang, Feng et al., 2021; J. S. Wang, Li et al., 2021).

XFZYD is a representative formula for the treatment of internal stasis of blood (Han, 2020). In this formula, *Prunus davidiana* (Carrière) Franch (Rosaceae), *Carthamus tinctorius* L (Asteraceae), *Angelica sinensis* (Oliv.) Diels (Umbelliferae), and *Ligusticum striatum*

DC (Umbelliferae) are used to invigorate the blood and dispel stasis, so that the stasis can be removed without harming the blood. *Bupleurum chinense* DC (Umbelliferae) and *Citrus × aurantium* L (Rutaceae) clear the liver and Qi, so that Qi can move the blood. *Rehmannia glutinosa* (Gaertn.) DC (Araliaceae) cools the blood and clears heat, while *Angelica sinensis* invigorates the blood and moistens dryness, so that the stasis is removed without harming Yin (Li et al., 2022). The plant name has been checked with MPNS (<http://mpns.kew.org>). Ancient scholars of the Qing Dynasty in China often applied XFZYD to treat asthma (Zhang, 1977). In addition, modern research has demonstrated that XFZYD promotes angiogenesis, improves hypoxia tolerance, regulates blood lipids, inhibits platelet aggregation, and thus improves asthma disease (Z. D. Wu et al., 2000; J. H. Wu & Chen, 2013). Chinese medicine believes that the ultimate pathogenesis of ED is blood stasis, and XFZYD is a good formula to activate blood stasis; therefore, it has been used in clinical practice for many years to treat ED (J. S. Chen & Gao, 2017; F. Zhao, Zhao et al., 2018). In addition, in one study, patients with ED who received XFZYD had significantly higher scores on the 5-item International Index of Erectile Function scale than control subjects (Lin et al., 2018).

We used high-performance liquid chromatography-tandem mass spectrometry (HPLC-MS/MS) and network pharmacology analysis to identify potential targets of XFZYD, and used animal experiments to evaluate the effect of XFZYD on asthma-related ED to better elucidate the mechanism of action of XFZYD in the treatment of asthma-related ED.

Materials and Method

Full-Spectrum Metabolite Analysis

HPLC-MS/MS was employed for XFZYD component identification (W. Chen et al., 2013). The XFZYD was purchased from Dongzhimen Hospital of Beijing University of Chinese Medicine (BUCM), which was uniformly procured by the Pharmacy Department of Dongzhimen Hospital of BUCM from Beijing Kang Rentang Pharmaceutical Co Ltd. (Beijing, China) and was the same batch of pellets as the animal intervention. The sample underwent pretreatment, whereby it was dried and grinded into powder, prior to weighing and resuspension into a preset volume. The sample was then filtered and centrifuged to remove particles and passed through a C18 column (Zorbax eclipse C18 [1.8 μm \times 2.1 mm \times 100 mm] using Q exactive HF ultimate 3000 LC system; Thermo Fisher Scientific, Waltham, MA, USA) for analysis, at 30°C. The flow

Table 1. Plant Names

Chinese name	Family	English name	Accepted scientific name
Dang Gui	Umbelliferae	Angelica sinensis	<i>Angelica sinensis</i> (Oliv.) Diels
Sheng Di Huang	Araliaceae	Rehmannia glutinosa	<i>Rehmannia glutinosa</i> (Gaertn.) DC
Tao Ren	Rosaceae	Peach kernel	<i>Prunus davidiana</i> (Carrière) Franch
Hong Hua	Asteraceae	Safflower	<i>Carthamus tinctorius</i> L
Zhi Qiao	Rutaceae	Fructus aurantii	<i>Citrus × aurantium</i> L
Chi Shao	Ranunculaceae	Red peony	<i>Paeonia lactiflora</i> Pall
Chai Hu	Umbelliferae	Radix bupleuri	<i>Bupleurum chinense</i> DC
Chuan Xiong	Umbelliferae	Ligusticum wallichii	<i>Ligusticum striatum</i> DC
Jie Geng	Eustomaceae	Platycodon grandiflorum	<i>Platycodon grandiflorus</i> (Jacq.) A.DC
Niu Xi	Amaranthaceae	Radix achyranthis bidentatae	<i>Achyranthes bidentata</i> Blume

rate was 0.3 mL/min, and the mobile phases A and B were water +0.1% formic acid and pure acetonitrile, respectively. The injection volume was 2 μ L. The compound discoverer v3.1 software (Thermo Fisher Scientific, Waltham, MA, USA) was employed for the correction of retention duration and screening of extracted peaks. The compounds were identified through secondary mass spectrometry using mzcloud and mzvault databases (Thermo Fisher Scientific, Waltham, MA, USA). Compound Discoverer v3.0 software was also used to extract target information from the original data (positive and negative ion modes) after extracting the peaks (Garcia & Barbas, 2011).

Target Collection

We used the GeneCards (Rappaport et al., 2017) and Online Mendelian Inheritance in Man (OMIM) databases (<https://omim.org/>; Hamosh et al., 2005) to search for asthma- and ED-related targets. PubChem (<https://pubchem.ncbi.nlm.nih.gov/>) and Swiss target prediction (<http://old.swisstargetprediction.ch/>) were employed to obtain the targets of the active components of XFZYD collected in HPLC-MS.

Protein–Protein Interaction Network Analysis

Potential protein–protein interactions (PPIs) were identified using the String database (<https://string-db.org/>; Szklarczyk et al., 2017). The data underwent filtering with the smallest interaction score of 0.40 to augment data reliability. The subsequent PPI information was used for network building and analyses.

Network Construction and Analysis

Cytoscape v3.8.0 software (<https://cytoscape.org/>) was employed for the construction of herb–

compound–target–disease and PPI networks. Subsequently, the PPI network was further analyzed with the Cytoscape plugin CytoHubba to identify primary targets (Ma et al., 2020).

Gene Ontology Activity and Kyoto Encyclopedia of Genes and Genomes Pathways Enrichment Analyses

Gene ontology (GO) and Kyoto Encyclopedia of Genes and Genomes (KEGG) enrichment analysis databases were employed (DAVID, <https://david.ncifcrf.gov/>, version 6.8) to obtain large-scale and comprehensive biological annotation functional data for gene or protein activity, which was then utilized for identification of the most augmented biological annotation. We imported the common goals into the DAVID database to analyze the GO and KEGG networks (R. L. Zhao & He, 2018).

Plant Names

The detailed plant names of XFZYD are shown in Table 1.

Drugs and Reagents

The components of XFZYD are *Angelica sinensis*, with its root (9 g, no. 19011501), *Rehmannia glutinosa*, with its root (9 g, no. 19043301), Peach kernel, with its seed (12 g, no. 19012131), Safflower, with its flower (9 g, no. 19038641), Fructus aurantii, with its fruit (6 g, no. 19034622), Red peony, with its root (6 g, no. 19006741), Radix bupleuri, with its root (3 g, no. 19035581), *Ligusticum wallichii*, with its root (4.5 g, no. 19014661), Platycodon grandiflorum, with its root (4.5 g, no. 19015111), and Radix achyranthis bidentatae, with its root (9 g, no. 19006041). In the composition of XFXYT, *Angelica sinensis*, *Rehmannia*

glutinosa, Peach kernel, Safflower, Fructus aurantii, Red peony, Radix bupleuri, *Ligusticum wallichii*, Platycodon grandiflorum, Radix achyranthis bidentatae are dispensed in the ratio of 6:6:8:6:4:4:2:3:3:6. The concentration of the drug was 0.617 g/mL. The volume of the drug was 10 mL/kg by gavage.

We purchased ovalbumin (OVA) from Sigma-Aldrich (St. Louis, MO, USA; CAT. A5503). Aluminum hydroxide gel was obtained from Pierce Biotechnology (Shanghai, China; CAT. 77161). Sinopharm Chemical Reagent Co. (Shanghai, China) provided the pentobarbital sodium. We obtained the primers from Invitrogen (Shanghai, China). IL-6 (CAT. BS-20393R), VEGFA (CAT. BS-20393R), and TNF (CAT. BS-10802R) assay kits were provided by Bioss (Woburn, MA, USA). eNOS antibody (76198) was provided by Abcam (Cambridge, UK). Dihydroethidium (DHE; Sigma, D7008, Saint Louis, MO, USA), 2-(4-Amidinophenyl)-6-indolecarbamide dihydrochloride (DAPI, Biyuntian, C1002, Shanghai, China). Horseradish peroxidase-conjugated immunoglobulin G (H + L) and biotin (CAT. BS-0295G) were obtained from Bioss. Immunoway (Plano, TX, USA; CAT. YM3028) produced mouse monoclonal anti- β -actin antibody.

Experimental Animals

Speyford (Beijing) Biotechnology Co., Ltd. (Beijing, China) (license number SCXK [Beijing] 2016-0002) provided 40 specific pathogen-free male Sprague-Dawley rats, which were maintained at the BUCM under a 12-hr light/dark cycle and 55% to 60% humidity at 22°C to 26°C. The rats were 4 to 5 weeks old and weighed 220 to 230 g. All rats were conditioned with deionized water and solid feed under these conditions for 7 days. Using the mating-behavior test and the noncontact penile erection test before experiments, we confirmed that the rats had normal sexual function (Jia et al., 2020). Experimental Animal Ethics Sub Committee of the Academic Committee of BUCM provided ethical approval for the in vivo experiments (BUCM-4-2019091105-3064).

Establishment of a Rat Model of Asthma and Screening of the ED Model

The sample size was determined using a resource equation calculation scheme with the formula: $E = N - K = Kn - K = K(n - 1)$ (Arifin & Zahiruddin, 2017). Where N is the total number of experimental units, n is the sample size of each group, K is the number of treatment groups, and E is the difference

between the two. The number of treatment groups in this study is four, so $\text{Max } N = \text{Max } n \times K = (20 / 4 + 1) \times 4 = 24$. Since four is an even number, the treatment groups are six rats each, and the corresponding blank group is six rats, for a total of 30 rats. The experiment needs to consider the attrition rate due to model failure, animal death, so the total number of animals in the experiment is 40. All 40 rats were assigned a number, and their body weights were recorded. A random number table was used to select 30 rats at random for the asthma model, whereas the normal group consisted of the remaining 10 rats.

According to the design principles of animal models, the replicated animal model should strive to reliably reflect human diseases, that is, it can specifically and reliably reflect a certain disease or a certain function, metabolism, or structural changes, and it should have the main symptoms and signs of the disease. Therefore, rats in the asthma model group were sensitized intraperitoneally on days 0, 7, and 14 with 1 mL of miscible liquid containing OVA (100 mg) and aluminum hydroxide gel (10 mg). The normal group of rats received an intraperitoneal (i.p.) injection of 1 mL of sterile physiological saline (0.9%) daily for the first 3 weeks of the experiment. Since day 22, normal and asthma model rats received sterile saline and 1% OVA, respectively, by inhalation through a compression nebulizer (NE-C900; Omron, Kyoto, Japan) at a rate of 0.2 mL/min for 30 min (Broide et al., 1998; Xiong et al., 2019). The rats in the asthma model group were then assessed for behavior, piloerection, dyspnea, nose scratching, incontinence, and diaphragmatic breathing after this procedure was repeated daily for 3 weeks (Z. R. Wang et al., 2018). After completion of the observations, rats in each group were fasted for 12 hr and then anesthetized with 1% sodium pentobarbital (30 mg/kg body weight), blood was collected from the abdominal aorta, and the rats were bled and executed. Then, three rats in the asthma model group and the normal group were randomly selected and pathological sections of their lungs were used for model evaluation.

Asthma model rats were weighed and placed in a quiet, dimly lit observation box for 10 min. Apomorphine (APO, 100 μ g/kg) was subcutaneously injected into the neck of every rat. The behavior of each rat was recorded on a video camera for 30 min after injection to see if penile erection—defined as the protrusion, swelling, or growth of the penis—took place (Park et al., 2018). Twenty-four of the 27 rats in the asthma model group reduced the number of erections, and these rats were diagnosed with asthma-related ED. Twenty-four rats were arbitrarily

separated into the asthma model group (Group M, $n = 6$), low-dose XFZYD group (Group D, $n = 6$), medium-dose XFZYD group (Group Z, $n = 6$), high-dose XFZYD group (Group G, $n = 6$), and the normal rats served as the control group (Group C, $n = 6$). Group C and Group M rats were administered deionized water via gavage; Group D rats were administered by gavage 3.09 g/kg XFZYD granule suspension was made in deionized water ($3 \times$ the human dose); Group Z rats were administered by gavage 6.17 g/kg XFZYD granule suspension prepared with deionized water ($6 \times$ the human dose); and Group G rats were administered by gavage 12.34 g/kg XFZYD granule suspension prepared with deionized water ($12 \times$ the human dose), with drug intervention for 8 weeks. All rats were routinely fed and administered once at 10:00 a.m. daily, and corresponding drugs were given via gavage according to the standard of 10 mL/kg body weight. The experimental group of rats underwent APO erectile induction and penile erection recording after 8 weeks of drug intervention. The procedure followed the same guidelines as the model screening stage. The indicators of humane endpoints are the following six: (1) persistent recumbency or inability of the rat to get up or walk; (2) persistent anorexia or 20% weight loss in 3 days; (3) excessive or prolonged hyperthermia or hypothermia; (4) diarrhea lasting 2 to 3 days; (5) genital or rectal prolapse; and (6) difficulty breathing or walking due to fluid in the abdomen.

Reactive Oxygen Species Analysis

At the end of the experiment, rats in each group were fasted for 12 hr, then anesthetized with 1% sodium pentobarbital (30 mg/kg body weight). The euthanasia used in this experiment was the bloodletting execution method, and blood was collected from the abdominal aorta and bled to sacrifice the rats. Frozen sections of penile tissue were thawed, and histochemical strokes were drawn surrounding the tissue to keep liquid from spreading. DHE was diluted in phosphate buffer saline (PBS), and the tissue was incubated with the dye at 37°C for 30 min without light. Then, the slides were incubated in PBS (pH 7.4) on a destaining shaker. After washing thrice in the dark (5 min each time), the sections were dried lightly, prior to DAPI staining and incubation at room temperature for 10 min without light for nuclear staining. The slides were PBS rinsed (pH 7.4) thrice on a destaining shaker in the dark (5 min each time). Next, they underwent mounting with an antifluorescence quenching mounting medium, prior to observation with a Nikon fluorescence microscope, and photography.

Histological Analysis

The middle region of the penile tissue was fixed in 4% paraformaldehyde and incubated in a dehydration box. Subsequently, the specimen was subjected to series-based alcoholic dehydration, wax-block embedding, slicing, xylene dewaxing, hematoxylin staining, alcohol differentiation, rinsing, anhydrous ethanol-based dehydration, eosin staining, xylene clearing, neutral resin fixation, and microscopic imaging.

Detection of IL-6, VEGFA, TNF, and eNOS Protein Levels by Western Blotting

Expression levels of IL-6, VEGFA, TNF, and eNOS in penile tissues were determined with western blotting. Penile tissue samples were obtained, weighed, homogenized in the radioimmunoprecipitation assay buffer on an ice bath, and centrifuged. After centrifugation for 10 min, the supernatant was taken out and BCA protein quantitative assay kit (GPP1815, GenePool) was applied to determine the protein concentrations. The SDS-PAGE gel was prepared, and the protein was added to the sample well using a microsampler. Protein samples were then separated by electrophoresis and transferred to polyvinylidene fluoride (PVDF) membranes. After blocking membranes with 5% bovine serum albumin (BSA), the primary antibodies of IL-6 (rabbit, bs-4539R, AB_11047924, 1:500, Bioss), VEGFA (rabbit, ab214424, AB_3064726, 1:500, Abcam), TNF (rabbit, ab205587, AB_2889389, 1:500, Abcam), eNOS (mouse, 76198, AB_1310183, 1:500, Abcam), and β -actin (mouse, ab6276, AB_2223210, 1:3,000, Abcam) were incubated with membranes over night at 4°C. Subsequently, the relevant second antibody Goat Anti-Rabbit IgG, HRP (ab6721, AB_955447, 1:5,000, Abcam) or Goat Anti-Mouse IgG, HRP (ab6789, AB_955439, 1:5,000, Abcam) was used to incubate the above membranes for 2 hr. The protein signals were observed by the enhanced chemiluminescence (ECL) reagents (GPP1824, GenePool). An automatic chemiluminescence imaging system was used to visualize protein bands (Y. T. Huang et al., 2019).

Real-Time Quantitative Polymerase Chain Reaction

Penile tissues were placed in a mortar and grinded rapidly thrice. Subsequently, 1 mL of the TRIzol reagent was added to extract total RNA. The isolated RNA was quantified and reverse-transcribed to cDNA using a reverse transcription kit. Target gene products were amplified as follows: predenaturation at 95°C for 15 min, denaturation at 95°C for 10 s, annealing, and

Table 2. The Primer Sequences for RT-qPCR

Primer name		Primer pairs (5' to 3')	Fragment length (bp)	Annealing temperature (°C)
IL6	Forward	CTCACGCACCGATGTCT	109	64.2
	Reverse	AGGCTGTGGGCTCAATC		64.3
VEGFA	Forward	CATCAAGCTCTCTCCTCCA	91	63.2
	Reverse	GGCCTCTTCTTCCACCA		63.5
TNF	Forward	CAGCCAGGAGGGAGAAC	93	63.9
	Reverse	GTATGAGAGGGACGGAACC		63.9
eNOS	Forward	CCATCATGGACCACCACACA	83	60
	Reverse	GGACCAGCCAAATCCAGTCT		60
β -actin	Forward	CCTCACTGTCCACCTTCCA	120	66
	Reverse	GGGTGAAAACGCAGCTCA		65

extension at 60°C for 30 s for 40 reactions. Subsequently, $2^{-\Delta\Delta C_t}$ values were calculated. The relative target gene expression was quantified and compared with the endogenous control β -actin gene expression. Table 2 displays the primer sequences used in this experiment.

Statistical Analyses

All data analyses employed SPSS 22.0 software. Data with normal distribution are presented as mean \pm standard deviation. Homogeneous variance data were assessed using one-way ANOVA, and intergroup pairwise comparison was done via the least significant difference test. Nonparametric rank-sum tests were employed for data with nonnormal distribution. Unordered count data were assessed via the chi-square test. $p < .05$ indicated statistical significance.

Results

Full-Spectrum Analyses of Metabolites

The HPLC-MS/MS full-spectrum analysis of XFZYD yielded 173 compounds. Table 3 displays the qualitative data for the metabolites.

Target Identification, Construction of a PPI Network, and Topologic Analysis

We identified 994 XFZYD targets using PubChem and Swiss Target Prediction and 500 asthma-related and 500 ED-related targets using GeneCards. Forty-one targets with XFZYD, asthma, and ED overlap (Figure 1A). We further analyzed 41 overlapping targets through network construction using the String database. Cytoscape was used to construct a PPI network (Figure 1B). The top 10 targets of the degree parameter according to the Cytoscape cytoHubba

plugin were albumin (ALB), IL-6, VEGFA, TNF, IL-1B, chemokine (C-X-C motif) ligand (CXCL)8, angiotensin I-converting enzyme, coagulation factor II, IL-2, and beta-2 adrenergic receptor (Figure 1C and Table 4). The key targets were ALB, IL-6, VEGFA, and TNF. Cytoscape was employed for traditional Chinese medicine (TCM) compound–target–disease network generation (Figure 2).

GO and KEGG Pathway Enrichment Analyses

Forty-one targets were analyzed using DAVID v6.8, which involved 200 cell biological processes (BP), 22 cellular components (CC), 26 molecular functions (MF), and 41 signaling networks (SN). Figure 3 illustrates the five leading BP and SN based on p values.

Validation of the Rat Asthma Model

The rats in the asthma model group displayed anxiety, piloerection, dyspnea, diaphragmatic breathing, nose scratching, and incontinence. The control rats did not show any of these symptoms. HE staining results showed that the alveolar walls of the rats in the control group were clear and complete, the bronchial lumen was regular, the smooth muscle and blood vessel walls were not significantly thickened, and there was no obvious inflammatory cell infiltration. Incomplete alveolar walls, massive infiltration of inflammatory cells around the trachea and in the pulmonary interstitium, and thickening of smooth muscle and vascular walls were all present in the rats in the model group's lung tissue (Figure 4).

Erection Time After XFZYD Treatment

The erection amount in Group M (0.67 ± 0.51) was markedly reduced, compared with Group C (2.33 ± 0.52 ; $p < .05$). After treatment with XFZYD, Groups

Table 3. Ingredient Separation and Identification of Xuefu Zhuyu Decoction Medicine by HPLC-MS

tR (min)	Name	Formula	Δ ppm	Ion species	Theoretical molecular weight
4.567	5'-S-methyl-5'-thioadenosine	C11H15N5O3S	0	[M+H] ⁺	297.08956
11.779	Ibuprofen	C12H16O2	0	[M+H] ⁺	192.11503
11.962	Dimefuron	C15H19ClN4O3	1	[M+H] ⁺	338.11457
0.878	N-(2,4-Dimethylphenyl)formamide	C9H11NO	0	[M+H] ⁺	149.08406
0.821	Betaine	C5H11NO2	0	[M+H] ⁺	117.07898
0.804	Boc-Asp-OH	C9H15NO6	-1	[M+H] ⁺	233.08994
0.875	D-(+)-pipercolinic acid	C6H11NO2	0	[M+H] ⁺	129.07898
0.869	Argininosuccinic acid	C10H18N4O6	-1	[M+H] ⁺	290.12263
1.227	3-Methylhippuric acid	C10H11NO3	0	[M+H] ⁺	193.07389
6.467	Cyclo(leucylprolyl)	C11H18N2O2	0	[M+H] ⁺	210.13683
1.423	L-Norleucine	C6H13NO2	0	[M+H] ⁺	131.09463
0.844	DL- β -Leucine	C6H13NO2	0	[M+H] ⁺	131.09463
0.832	D-(+)-Proline	C5H9NO2	1	[M+H] ⁺	115.06333
0.855	DL-Stachydrine	C7H13NO2	0	[M+H] ⁺	143.09463
1.15	4-Guanidinobutyric acid	C5H11N3O2	0	[M+H] ⁺	145.08513
1.269	L-Tyrosine	C9H11NO3	0	[M+H] ⁺	181.07389
2.334	L-Phenylalanine	C9H11NO2	0	[M+H] ⁺	165.07898
1.152	N-Acetylhistamine	C7H11N3O	0	[M+H] ⁺	153.09021
0.76	DL-Arginine	C6H14N4O2	0	[M+H] ⁺	174.11168
1.328	L-Isoleucine	C6H13NO2	0	[M+H] ⁺	131.09463
1.176	L-Pyroglutamic acid	C5H7NO3	0	[M+H] ⁺	129.04259
1.274	2-Hydroxycinnamic acid	C9H8O3	0	[M+H] ⁺	164.04734
6.642	4-Coumaric acid	C9H8O3	0	[M+H] ⁺	164.04734
6.962	Scopoletin	C10H8O4	0	[M+H] ⁺	192.04226
4.554	7-Hydroxycoumarin	C9H6O3	0	[M+H] ⁺	162.03169
1.982	Metharbital	C9H14N2O3	0	[M+H] ⁺	198.10044
1.175	Uracil	C4H4N2O2	1	[M+H] ⁺	112.02728
12.361	Bis(4-ethylbenzylidene)sorbitol	C24H30O6	-1	[M+H] ⁺	414.20424
17.017	Oleamide	C18H35NO	-1	[M+H] ⁺	281.27186
13.706	9-Oxo-10(E),12(E)-octadecadienoic acid	C18H30O3	-1	[M+H] ⁺	294.21949
9.963	9-Oxo-ODE	C18H30O3	-1	[M+H] ⁺	294.21949
0.852	S(8)-(2-methylpropanoyl)dihydrolipoamide	C12H23NO2S2	-4	[M+H] ⁺	277.11702
7.098	Naringin	C27H32O14	0	[M+H] ⁺	580.17921
10.645	Icaritin	C21H20O6	-1	[M+H] ⁺	368.12599
7.12	Kaempferol-7-O-glucoside	C21H20O11	-1	[M+H] ⁺	448.10056
11.185	Nobiletin	C21H22O8	-1	[M+H] ⁺	402.13147
8.107	Chrysin	C15H10O4	0	[M+H] ⁺	254.05791
9.779	Naringenin	C15H12O5	-1	[M+H] ⁺	272.06847
11.707	Tangeritin	C20H20O7	-1	[M+H] ⁺	372.1209
6.707	Hyperoside	C21H20O12	-1	[M+H] ⁺	464.09548
5.401	(-)-Epicatechin	C15H14O6	0	[M+H] ⁺	290.07904
7.326	Hesperidin	C28H34O15	0	[M+H] ⁺	610.18977
7.342	Hesperetin	C16H14O6	-1	[M+H] ⁺	302.07904
7.424	Diosmetin	C16H12O6	0	[M+H] ⁺	300.06339
7.299	Prunin	C21H22O10	-1	[M+H] ⁺	434.1213
6.65	Eriodictyol	C15H12O6	-1	[M+H] ⁺	288.06339
6.731	4',7-Dihydroxyflavanone	C15H12O4	-1	[M+H] ⁺	256.07356
10.006	3',5,7-Trihydroxy-4'-methoxyflavanone	C16H14O6	-1	[M+H] ⁺	302.07904
19.131	1-Stearoylglycerol	C21H42O4	-1	[M+H] ⁺	358.30831
0.819	Glycerophosphocholine	C8H20NO6P	-1	[M+H] ⁺	257.10282
1.154	Adenine	C5H5N5	0	[M+H] ⁺	135.0545
1.2	Guanine	C5H5N5O	0	[M+H] ⁺	151.04941
4.633	4-Indolecarbaldehyde	C9H7NO	0	[M+H] ⁺	145.05276
4.63	Trans-3-indoleacrylic acid	C11H9NO2	0	[M+H] ⁺	187.06333
4.592	Indole	C8H7N	1	[M+H] ⁺	117.05785
5.506	2,3,4,9-Tetrahydro-1H- β -carboline-3-carboxylic acid	C12H12N2O2	0	[M+H] ⁺	216.08988
12.449	Sedanolid	C12H18O2	0	[M+H] ⁺	194.13068
7.927	Senkyunolide H	C12H16O4	0	[M+H] ⁺	224.10486
8.99	5-O-Methylgenistein	C16H12O5	-1	[M+H] ⁺	284.06847
10.502	Formononetin	C16H12O4	0	[M+H] ⁺	268.07356

(continued)

Table 3. (continued)

tR (min)	Name	Formula	Δ ppm	Ion species	Theoretical molecular weight
7.865	Ononin	C22H22O9	0	[M+H] ⁺	430.12638
13.24	5,7,3',4'-Tetrahydroxy-6,8-diprenylisoflavone	C25H26O6	-1	[M+H] ⁺	422.17294
8.853	(5S,6S)-5-Hydroxy-4-methoxy-6- [(E)-2-phenylvinyl]-5,6-dihydro-2H-pyran-2-one	C14H14O4	-1	[M+H] ⁺	246.08921
11.796	Licochalcone A	C21H22O4	-1	[M+H] ⁺	338.15181
7.105	Naringenin-chalcone	C15H12O5	-1	[M+H] ⁺	272.06847
5.505	2-Naphthylamine	C10H9N	0	[M+H] ⁺	143.0735
0.827	Diethylpyrocarbonate	C6H10O5	-1	[M+H] ⁺	162.05282
0.829	Acetylcholine	C7H15NO2	0	[M+H] ⁺	145.11028
0.783	Choline	C5H13NO	2	[M+H] ⁺	103.09971
0.805	Muramic acid	C9H17NO7	-1	[M+H] ⁺	251.1005
5.49	Amygdalin	C20H27NO11	-1	[M+H] ⁺	457.15841
5.316	Chlorogenic acid	C16H18O9	0	[M+H] ⁺	354.09508
0.815	Galactinol	C12H22O11	-1	[M+H] ⁺	342.11621
9.704	5-Phenylcyclohexane-1,3-dione	C12H12O2	-1	[M+H] ⁺	188.08373
17.183	Muscone	C16H30O	-1	[M+H] ⁺	238.22967
0.779	Kanosamine	C6H13NO5	0	[M+H] ⁺	179.07937
0.84	Glucose 1-phosphate	C6H13O9P	-1	[M+H] ⁺	260.02972
0.8	D-Raffinose	C18H32O16	0	[M+H] ⁺	504.16903
1.377	Acetophenone	C8H8O	1	[M+H] ⁺	120.05751
11.513	N2-[2-(tert-Butylthio)ethyl]-4,6-bis(4-fluorophenoxy)- 1,3,5-triazin-2-amine	C21H22F2N4O2S	-3	[M+H] ⁺	432.14315
1.343	1,2-di-O-methyl-4-[(2R)-2,4-dihydrobutyramido]-4,6- dideoxy-alpha-D-mannopyranoside	C12H23NO7	-1	[M+H] ⁺	293.14745
0.818	Ethyl 4-(4-fluorophenyl)-2-[(tetrahydro-2- furanlylcarbonyl)amino]-3-thiophenecarboxylate	C18H18FNO4S	-3	[M+H] ⁺	363.09406
5.669	(S)-N-alpha-benzoylarginine ethyl ester	C15H22N4O3	-1	[M+H] ⁺	306.16919
9.903	(3beta,5xi,9xi)-3,23-Dihydroxy-1-oxoolean-12-en-28-oic acid	C30H46O5	-1	[M+H] ⁺	486.33452
7.105	7-Hydroxy-2-(4-hydroxyphenyl)-4-oxo-3,4-dihydro-2H- chromen-5-yl beta-D-glucopyranoside	C21H22O10	-1	[M+H] ⁺	434.1213
6.053	[(3R,5R,6S,8S)-3-(beta-D-Glucopyranosyloxy)-6-hydroxy-8- methyl-9,10-dioxatetracyclo[4.3.1.02,5.03,8]dec-2- yl]methyl benzoate	C23H28O11	-1	[M+H] ⁺	480.16316
1.152	5-(acetylamino)-2,6-anhydro-3,5-dideoxy-D-erythro-non-2- enonic acid	C11H17NO8	-1	[M+H] ⁺	291.09542
9.545	{(3R,5R,6S,8S)-3-[(6-O-Benzoyl-beta-D-glucopyranosyl)oxy]-6- hydroxy-8-methyl-9,10- dioxatetracyclo[4.3.1.02,5.03,8]dec-2-yl}methyl benzoate	C30H32O12	0	[M+H] ⁺	584.18938
0.801	DA9185000	C12H10O5	0	[M+H] ⁺	202.04524
1.186	Phloroglucinol	C6H6O3	0	[M+H] ⁺	126.03169
6.622	Vanillin	C8H8O3	0	[M+H] ⁺	152.04734
6.056	Coniferyl aldehyde	C10H10O3	-1	[M+H] ⁺	178.06299
10.9	Limonin	C26H30O8	0	[M+H] ⁺	470.19407
10.157	Glycyrrhizin	C42H62O16	0	[M+H] ⁺	822.40379
10.157	18-beta-Glycyrrhetic acid	C30H46O4	-1	[M+H] ⁺	470.33961
8.518	Berberine	C20H17NO4	-1	[M+H] ⁺	335.11576
1.252	Adenosine	C10H13N5O4	-1	[M+H] ⁺	267.09675
1.157	Adenosine 5'-monophosphate	C10H14N5O7P	-1	[M+H] ⁺	347.06308
1.152	3-Hydroxy-2-methylpyridine	C6H7NO	2	[M+H] ⁺	109.05276
1.179	6-Hydroxypicolinic acid	C6H5NO3	0	[M+H] ⁺	139.02694
0.835	Methyl isonicotinate	C7H7NO2	0	[M+H] ⁺	137.04768
6.729	Ecdysterone	C27H44O7	0	[M+H] ⁺	480.3087
0.868	Ecgonine methyl ester	C10H17NO3	0	[M+H] ⁺	199.12084
16.775	2,2'-Methylenebis(4-methyl-6-tert-butylphenol)	C23H32O2	0	[M+H] ⁻	340.24023
5.616	Isophthalic acid	C8H6O4	-4	[M+H] ⁻	166.02661
1.855	Gallic acid	C7H6O5	-4	[M+H] ⁻	170.02152
11.959	Dimefuron	C15H19ClN4O3	3	[M+H] ⁻	338.11457
9.776	Butylparaben	C11H14O3	-3	[M+H] ⁻	194.09429
1.275	L-Tyrosine	C9H11NO3	-3	[M+H] ⁻	181.07389
1.156	Citric acid	C6H8O7	-3	[M+H] ⁻	192.027

(continued)

Table 3. (continued)

tR (min)	Name	Formula	Δ ppm	Ion species	Theoretical molecular weight
5.787	Caffeic acid	C ₉ H ₈ O ₄	-3	[M+H] ⁻	180.04226
6.958	Ferulic acid	C ₁₀ H ₁₀ O ₄	-3	[M+H] ⁻	194.05791
4.904	Esculin	C ₁₅ H ₁₆ O ₉	0	[M+H] ⁻	340.07943
7.544	Azelaic acid	C ₉ H ₁₆ O ₄	-3	[M+H] ⁻	188.10486
15.977	Oleic acid alkylne	C ₁₈ H ₃₀ O ₂	0	[M+H] ⁻	278.22458
11.948	(+/-)12(13)-DiHOME	C ₁₈ H ₃₄ O ₄	0	[M+H] ⁻	314.24571
9.608	Corchorifatty acid F	C ₁₈ H ₃₂ O ₅	0	[M+H] ⁻	328.22497
5.762	{(1R,2R)-2-[(2Z)-5-(Hexopyranosyloxy)-2-penten-1-yl]-3-oxocyclopentyl}acetic acid	C ₁₈ H ₂₈ O ₉	1	[M+H] ⁻	388.17333
12.065	(+/-)9,10-dihydroxy-12Z-octadecenoic acid	C ₁₈ H ₃₄ O ₄	0	[M+H] ⁻	314.24571
7.1	Naringin	C ₂₇ H ₃₂ O ₁₄	0	[M+H] ⁻	580.17921
6.613	Licuroside	C ₂₆ H ₃₀ O ₁₃	1	[M+H] ⁻	550.16864
10.137	Hispidulin	C ₁₆ H ₁₂ O ₆	0	[M+H] ⁻	300.06339
9.778	Naringenin	C ₁₅ H ₁₂ O ₅	0	[M+H] ⁻	272.06847
6.706	Quercetin-3 β -D-glucoside	C ₂₁ H ₂₀ O ₁₂	1	[M+H] ⁻	464.09548
8.894	Eriodictyol	C ₁₅ H ₁₂ O ₆	0	[M+H] ⁻	288.06339
5.405	Catechin	C ₁₅ H ₁₄ O ₆	0	[M+H] ⁻	290.07904
10.006	3',5,7-Trihydroxy-4'-methoxyflavanone	C ₁₆ H ₁₄ O ₆	0	[M+H] ⁻	302.07904
6.517	2-(6-Hydroxyhexyl)-3-methylenesuccinic acid	C ₁₁ H ₁₈ O ₅	0	[M+H] ⁻	230.11542
4.642	DL-Tryptophan	C ₁₁ H ₁₂ N ₂ O ₂	-2	[M+H] ⁻	204.08988
10.5	Formononetin	C ₁₆ H ₁₂ O ₄	0	[M+H] ⁻	268.07356
6.733	3'-C-Glucosylisoliquiritigenin	C ₂₁ H ₂₂ O ₉	1	[M+H] ⁻	418.12638
5.824	Phlinoside A	C ₃₅ H ₄₆ O ₂₀	2	[M+H] ⁻	786.25824
7.339	4,5-Dicaffeoylquinic acid	C ₂₅ H ₂₄ O ₁₂	0	[M+H] ⁻	516.12678
6.183	D(-)-Amygdalin	C ₂₀ H ₂₇ NO ₁₁	0	[M+H] ⁻	457.15841
5.319	Chlorogenic acid	C ₁₆ H ₁₈ O ₉	1	[M+H] ⁻	354.09508
0.789	Stachyose	C ₂₄ H ₄₂ O ₂₁	0	[M+H] ⁻	666.22186
7.495	Lusitanicoside	C ₂₁ H ₃₀ O ₁₀	1	[M+H] ⁻	442.1839
9.224	4-(4-Ethoxyphenyl)-4-oxobutanoic acid	C ₁₂ H ₁₄ O ₄	-1	[M+H] ⁻	222.08921
0.821	Sucrose	C ₁₂ H ₂₂ O ₁₁	0	[M+H] ⁻	342.11621
0.85	D-(+)-Xylose	C ₅ H ₁₀ O ₅	-4	[M+H] ⁻	150.05282
0.791	D(-)-Mannitol	C ₆ H ₁₄ O ₆	-3	[M+H] ⁻	182.07904
0.833	D(-)-Quinic acid	C ₇ H ₁₂ O ₆	-3	[M+H] ⁻	192.06339
0.833	D-Saccharic acid	C ₆ H ₁₀ O ₈	-2	[M+H] ⁻	210.03757
5.456	Neochlorogenic acid	C ₁₆ H ₁₈ O ₉	1	[M+H] ⁻	354.09508
0.856	D-Glucono-1,5-lactone	C ₆ H ₁₀ O ₆	-2	[M+H] ⁻	178.04774
5.487	[(6-O-Hexopyranosylhexopyranosyl)oxy](phenyl)acetonitrile	C ₂₀ H ₂₇ NO ₁₁	1	[M+H] ⁻	457.15841
1.86	Sibiricoside A3	C ₁₉ H ₂₆ O ₁₃	1	[M+H] ⁻	462.13734
4.565	Bioside	C ₂₀ H ₃₀ O ₁₂	1	[M+H] ⁻	462.17373
6.188	(3R,5R)-1,3,5-Trihydroxy-4-[[2(E)-3-(4-hydroxy-3-methoxyphenyl)-2-propenyl]oxy]cyclohexanecarboxylic acid	C ₁₇ H ₂₀ O ₉	0	[M+H] ⁻	368.11073
12.768	N-(3-Chloro-4-morpholinophenyl)-6-oxo-1,4,5,6-tetrahydro-3-pyridazinecarboxamide	C ₁₅ H ₁₇ CIN ₄ O ₃	4	[M+H] ⁻	336.09892
5.694	3,4-Dihydroxyphenylacetic acid	C ₈ H ₈ O ₄	-4	[M+H] ⁻	168.04226
6.75	D(+)-Phenyllactic acid	C ₉ H ₁₀ O ₃	-4	[M+H] ⁻	166.06299
6.32	Agnuside	C ₂₂ H ₂₆ O ₁₁	1	[M+H] ⁻	466.14751
10.153	Glycyrrhizin	C ₄₂ H ₆₂ O ₁₆	1	[M+H] ⁻	822.40379
6.257	Paeoniflorin	C ₂₃ H ₂₈ O ₁₁	0	[M+H] ⁻	480.16316
6.053	Albiflorin	C ₂₃ H ₂₈ O ₁₁	0	[M+H] ⁻	480.16316
13.969	18- β -Glycyrrhetic acid	C ₃₀ H ₄₆ O ₄	0	[M+H] ⁻	470.33961
4.627	Mussaenosidic acid	C ₁₆ H ₂₄ O ₁₀	0	[M+H] ⁻	376.13695
1.174	Guanosine monophosphate	C ₁₀ H ₁₄ N ₅ O ₈ P	0	[M+H] ⁻	363.058
0.845	Cabotegravir	C ₁₉ H ₁₇ F ₂ N ₃ O ₅	-4	[M+H] ⁻	405.11363
1.183	Uridine	C ₉ H ₁₂ N ₂ O ₆	0	[M+H] ⁻	244.06954
0.867	N-[4-(2-Pyrimidinylsulfamoyl)phenyl]benzamide	C ₁₇ H ₁₄ N ₄ O ₃ S	3	[M+H] ⁻	354.07866
0.803	(2E)-3-[3-(Trifluoromethyl)phenyl]acrylic acid	C ₁₀ H ₇ F ₃ O ₂	0	[M+H] ⁻	216.03981
0.877	5-(acetylamino)-2,6-anhydro-3,5-dideoxy-L-glycero-L-altro-non-2-enonic acid	C ₁₁ H ₁₇ NO ₈	0	[M+H] ⁻	291.09542
5.039	4-Acetyl-3-hydroxy-5-methylphenyl β -D-glucopyranoside	C ₁₅ H ₂₀ O ₈	1	[M+H] ⁻	328.11582

(continued)

Table 3. (continued)

tR (min)	Name	Formula	Δ ppm	Ion species	Theoretical molecular weight
5.354	3-[2-(β -D-Glucopyranosyloxy)-4-methoxyphenyl]propanoic acid	C16H22O9	0	[M+H] ⁻	358.12638
0.814	MFCD01051705	C17H19ClN4O2S	3	[M+H] ⁻	378.09172
7.365	7-Hydroxy-2-(4-hydroxyphenyl)-4-oxo-3,4-dihydro-2H-chromen-5-yl β -D-glucopyranoside	C21H22O10	0	[M+H] ⁻	434.1213
3.178	2-[(5-Benzyl-6-methyl-4-oxo-1,4-dihydro-2-pyrimidinyl)sulfanyl]-N-(1,5-dimethyl-3-oxo-2-phenyl-2,3-dihydro-1H-pyrazol-4-yl)acetamide	C25H25N5O3S	3	[M+H] ⁻	475.16781
5.256	(1S,4aS,7S,7aS)-7-Hydroxy-1-[[6-O-(4-hydroxybenzoyl)- β -D-glucopyranosyl]oxy]-7-methyl-1,4a,5,6,7,7a-hexahydrocyclopenta[c]pyran-4-carboxylic acid	C23H28O12	0	[M+H] ⁻	496.15808
7.327	4,2',4'-Trihydroxy-6'-methoxychalcone 4,4'-di- β -glucoside	C28H34O15	1	[M+H] ⁻	610.18977
6.899	2-(3,4-Dihydroxyphenyl)ethyl 3-O-(6-deoxy- β -L-mannopyranosyl)-6-O-[(2E)-3-(3,4-dihydroxyphenyl)-2-propenoyl]- β -D-glucopyranoside	C29H36O15	1	[M+H] ⁻	624.20542
0.811	Butyl ({5-isobutyl-3-[4-({4-oxo-2-propyl-6-[(2-thienylcarbonyl)amino]-3(4H)-quinazolinyl]methyl}phenyl]-2-thienyl}sulfonyl)carbamate	C36H40N4O6S3	-1	[M+H] ⁻	720.211

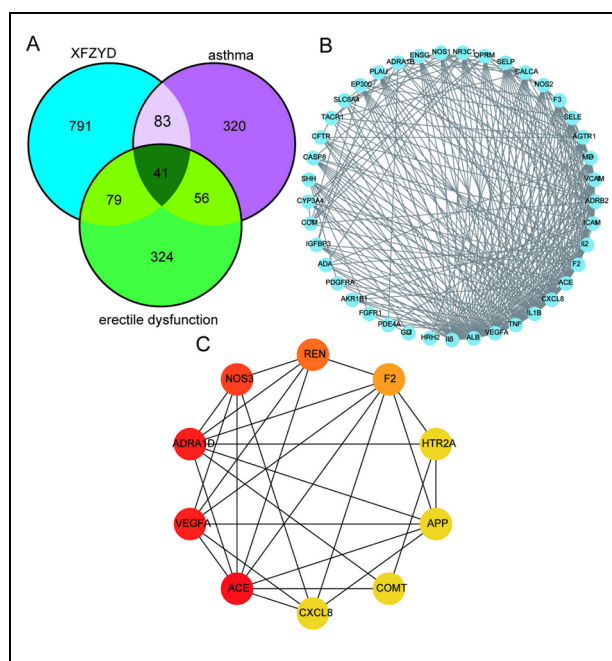


Figure 1. (A) Intersection of Xuefu Zhuyu Decoction Targets, Asthma Targets, and Erectile Dysfunction Targets; (B) PPI Network Built by Cytoscape (3.7.1); (C) PPI Network Processed by Cytoscape (3.7.1) Plugin (cytoHubba)

Z and G experienced significantly more erections (1.50 ± 0.55 ; 1.67 ± 0.52) than Group M ($p < .05$), and Group D experienced significantly more erections (1.17 ± 0.41) but without statistical significance ($p > .05$; Table 5).

Table 4. Key Target Genes as Determined by the CytoHubba Plugin in Cytoscape

Rank	Name	Score
1	Albumin (ALB)	28
2	Interleukin 6 (IL-6)	26
3	Vascular endothelial growth factor A (VEGFA)	24
4	Tumor necrosis factor (TNF)	24
4	Interleukin 1 beta (IL-1B)	23
6	C-X-C motif chemokine ligand 8 (CXCL8)	22
6	Angiotensin I converting enzyme (ACE)	22
6	Coagulation factor II, thrombin (F2)	22
9	Interleukin 2 (IL2)	21
9	Adrenoceptor beta 2 (ADRB2)	21

Reactive Oxygen Species Levels in Rats Following Drug Intervention

The content in Group M was markedly elevated, compared with Group C ($p < .05$). Following drug treatment, reactive oxygen species (ROS) levels in Groups D, Z, and G were obviously reduced, relative to Group M ($p < .05$; Figure 5).

Histologic Analysis of Corpus Caverosum

In Group C, cavernous trabeculae and evenly distributed blood sinuses were visible after corpus cavernosum tissue samples were stained with hematoxylin-eosin (HE) and examined under a light microscope. Red blood cells filled the sinus space, and endothelial cells

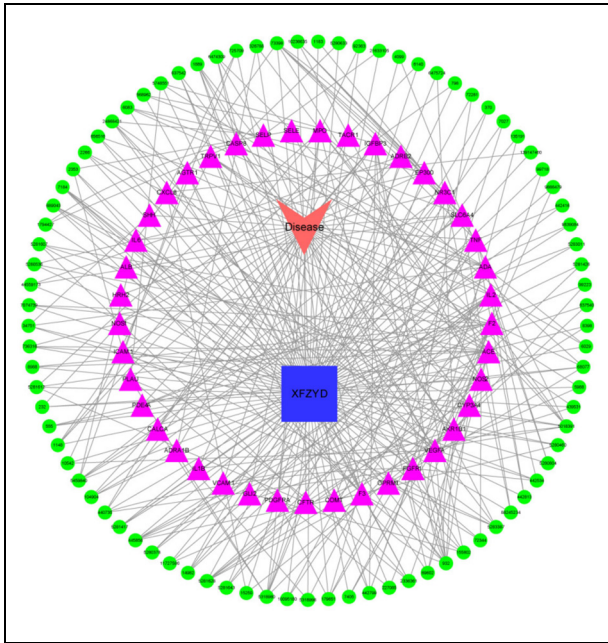


Figure 2. The Network Construction for Herbal-Compound-Targets-Disease

lined the inner wall. There was a lot of smooth muscle and a few small blood vessels in the trabecular sinus. The density of endothelial and smooth muscle cells was reduced. The distribution of blood sinusoids was disordered in Group M. Collagen fibers were also more in number than in Group C. After 8 weeks of XFZYD treatment, the blood sinusoids were distributed more regularly in Groups D, Z, and G than in Group M, endothelial cells density increased, and the number of collagen fibers was relatively decreased (Figure 6).

IL-6, VEGFA, TNF, and eNOS Expression Following XFZYD Treatment

Western blotting ($p < .05$) revealed that the levels of the proteins IL-6, VEGFA, and TNF in penile tissue were higher in Group M (0.95 ± 0.02 ; 1.16 ± 0.03 ; 1.11 ± 0.03) than in Group C (0.65 ± 0.03 ; 0.71 ± 0.03 ; 0.67 ± 0.02). The expression of all three proteins were downregulated in the D, Z, and G groups (0.88 ± 0.03 , 1.07 ± 0.03 , 0.95 ± 0.02 ; 0.74 ± 0.02 , 0.87 ± 0.02 , 0.77 ± 0.03 ; 0.71 ± 0.02 , 0.83 ± 0.03 , 0.74

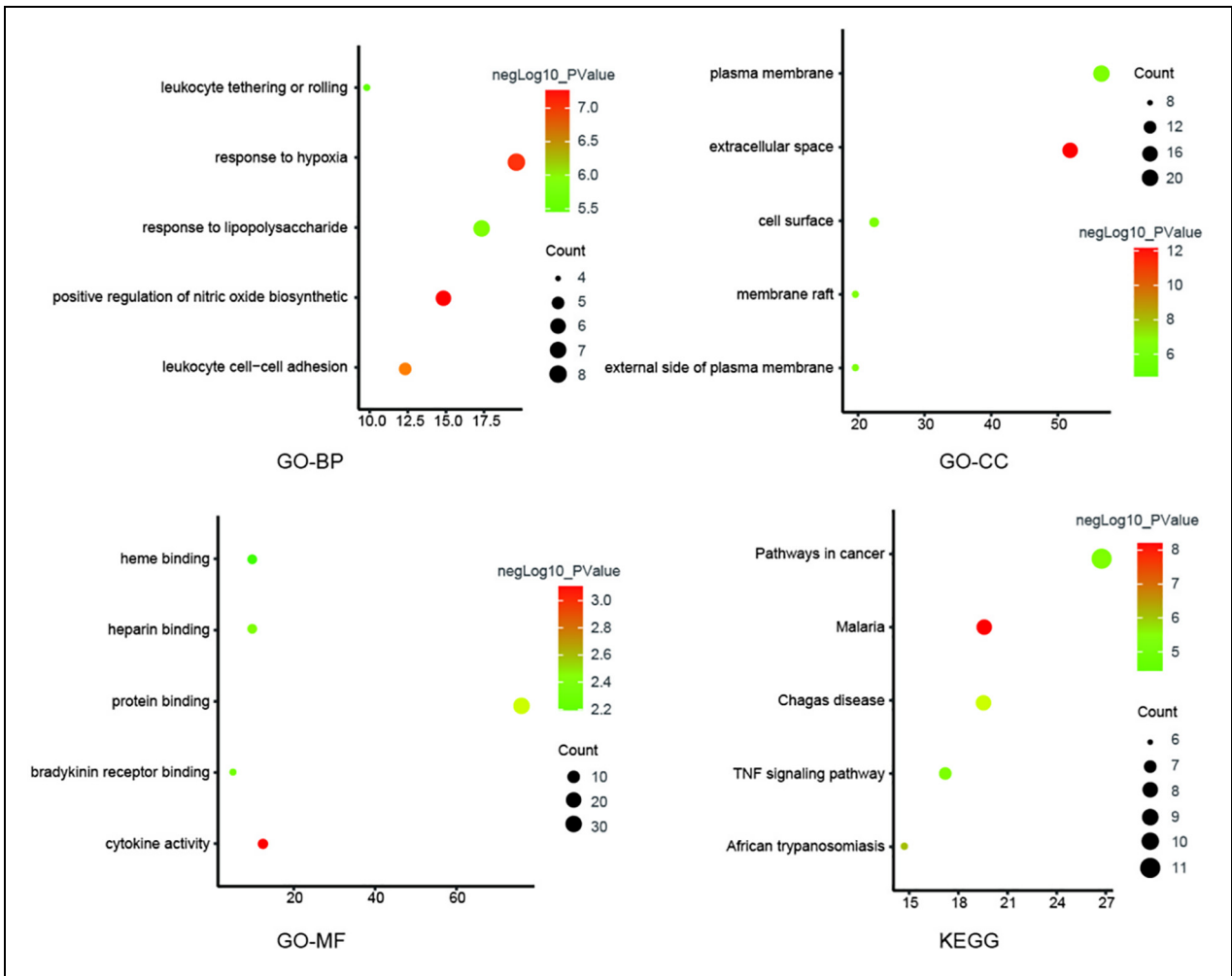


Figure 3. Analyses of Pathway Enrichment Using GO and KEGG Databases

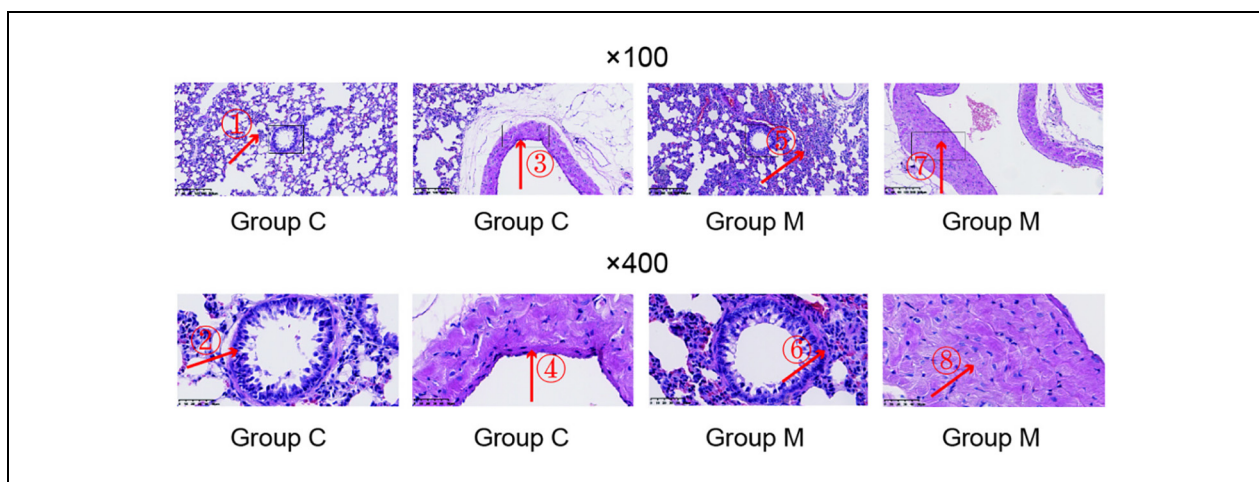


Figure 4. HE Staining of Lung Tissue in Groups C and M ($\times 100$ and $\times 400$). (A) In Group C: The Alveolar Walls Were Clear and Complete, the Bronchial Lumen Was Regular, the Smooth Muscle and Blood Vessel Walls Were Not Significantly Thickened, and There Was No Obvious Inflammatory Cell Infiltration (Arrows ①②③④). (B) In Group M: The Lung Tissue Structure Was Disordered, Incomplete Alveolar Walls, Massive Infiltration of Inflammatory Cells Around the Trachea and in the Pulmonary Interstitium, and Thickening of Smooth Muscle and Vascular Walls (Arrows ⑤⑥⑦⑧)

Table 5. Erectile Times of Rats in Each Group After Drug Intervention

Group	N	Erectile times
C	6	2.33 ± 0.52
M	6	$0.67 \pm 0.51^*$
D	6	1.17 ± 0.41
Z	6	$1.50 \pm 0.55^{**}$
G	6	$1.67 \pm 0.52^{**}$

Note. Differences with $p < .05$ were considered statistically significant. * $p < .05$, the M group versus the C group; ** $p < .05$, the Z and G groups versus the M group.

± 0.02) than Group M ($p < .05$). eNOS protein levels in Group M (0.12 ± 0.04) were drastically reduced, compared with Group C (0.69 ± 0.04 ; $p < .05$). After drug treatment, eNOS protein levels in the D, Z, and G groups (0.34 ± 0.03 ; 0.48 ± 0.04 ; 0.56 ± 0.02) were markedly higher, compared with Group M ($p < .05$; Figure 7A and 7B). The mRNA levels of IL-6, VEGFA, TNF, and eNOS showed similar trends (Group M: 1.93 ± 0.12 , 1.54 ± 0.12 , 2.95 ± 0.09 , 0.22 ± 0.06 ; Group D: 1.77 ± 0.07 , 1.45 ± 0.06 , 2.75 ± 0.06 , 0.60 ± 0.05 ; Group Z: 1.36 ± 0.08 , 1.25 ± 0.04 , 1.72 ± 0.07 , 0.80 ± 0.06 ; Group G: 1.33 ± 0.07 , 1.23 ± 0.03 , 1.51 ± 0.05 , 0.87 ± 0.05 ; all $p < .05$; Figure 7C).

Discussion

There have been few studies on ED in patients with asthma, and it is unclear what causes the two

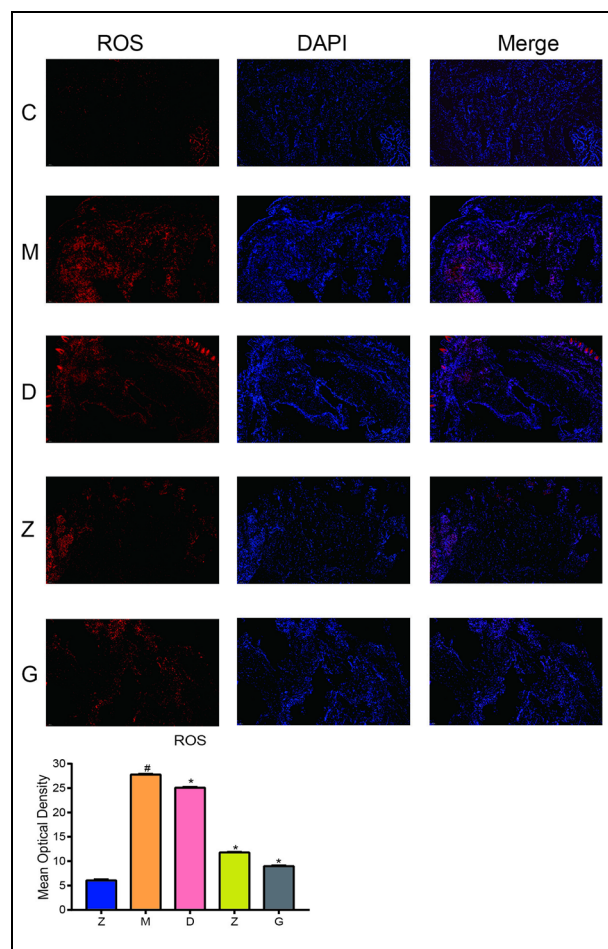


Figure 5. ROS Levels in Rats in Each Group After Drug Intervention ($\times 100$, Black = 5, Gamma = 1, White = 255)

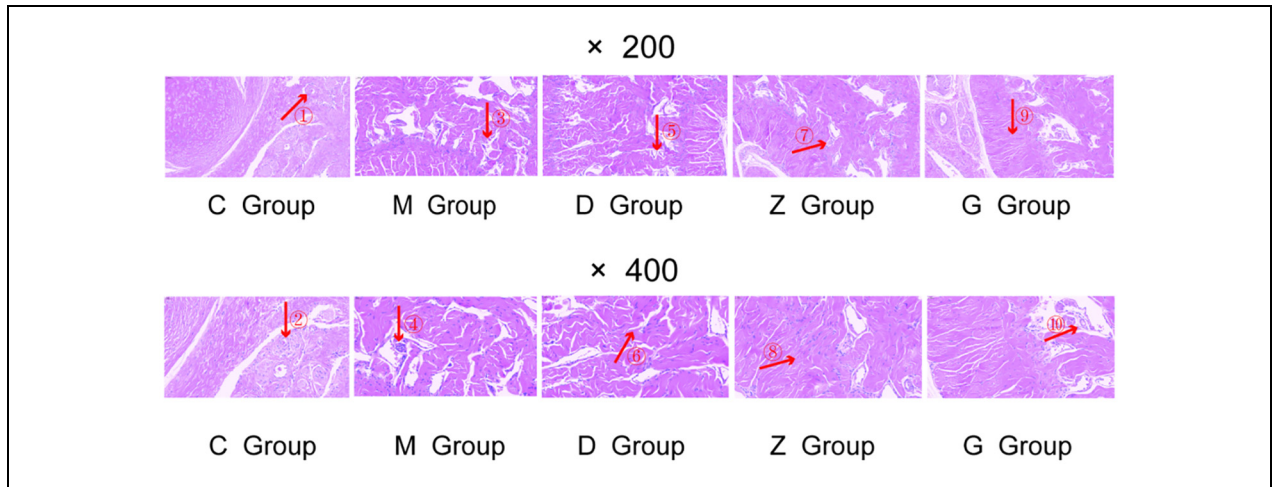


Figure 6. HE Staining of Penile Tissue of Rats From the C, M, and T Groups ($\times 200$ and $\times 400$). (A) In the C Group: The Blood Sinuses Were Evenly Distributed, With Red Blood Cells in the Sinus Space and Endothelial Cells Covering the Inner Wall (Arrows ①②). (B) In the M Group: The Distribution of Blood Sinusoids Was Disordered, and the Density of Endothelial Cells and Smooth Muscle Cells Was Reduced (Arrows ③④). (C) In the D, Z, and G Group: The Distribution of Blood Sinuses Was More Regular and the Density of Endothelial Cells Was Increased, the Number of Collagen Fibers Was Relatively Reduced (Arrows ⑤⑥⑦⑧⑨⑩).

conditions to coexist. In this study, XFZYD was found to enhance erectile function in asthmatic rats. Our network pharmacology analysis identified ALB, IL-6, VEGFA, and TNF as potential XFZYD targets. However, previous studies revealed that the ALB protein expression in an asthma-associated ED model and the control did not differ (J. S. Wang et al., 2020). Therefore, we focused on IL-6, VEGFA, and TNF in our study as potential mediators of the beneficial effects of XFZYD on asthma-associated ED.

The inflammatory response and immune regulation of asthma, including its induction and exacerbation, are significantly influenced by inflammatory mediators. The proinflammatory cytokine IL-6, produced mainly by monocytes and macrophages, has been implicated in bronchial asthma, and its detection is useful in evaluating the condition and tracking the effectiveness of treatment (Siwiec et al., 2009). Overexpression of IL-6 during immune response and inflammation can enhance the proliferation and differentiation of different cell types, which can alter erectile function (Proboszcz et al., 2017). TNF- α is an inflammatory cytokine associated with type-1 helper T cells that have been linked to the pathogenesis of asthma (Cazzola & Polosa, 2006). TNF increases vascular permeability and activates T cells, eosinophils, and mast cells as neutrophil and monocyte chemokine (Diouf et al., 2007). The peripheral blood TNF level of patients with asthma was shown to be elevated than that of patients without asthma, which was positively correlated with the severity of the disease.

A potential risk factor for the pathophysiological process of ED is low-grade systemic inflammation. The inflammatory process of ED involves the transformation of complex interactions between cytokines, chemokines, and adhesion molecules. Numerous clinical studies have shown a strong correlation between the increased expression of clinical inflammatory markers and mediators and the occurrence and development of ED (Araña Rosáinz Mde et al., 2011; Vlachopoulos et al., 2006). Proinflammatory and inflammatory cytokines are primarily responsible for completing the inflammatory response. The body produces a variety of proinflammatory cytokines, including IL-6, TNF- α , and so on (Zimmerman, 2002). The occurrence of asthma increases IL-6, TNF- α proinflammatory cytokines, and inhibits eNOS and activity. NO is a powerful smooth muscle relaxation factor, and eNOS is the key enzyme to generate NO. Any cause that reduces eNOS activity and thus NO production could be the pathogenesis of ED (Musicki & Burnett, 2006). Studies have shown that eNOS is localized in vascular endothelial cells and smooth muscle cells in the corpus cavernosum of the rat penis and plays an important role in the relaxation of the corpus cavernosum (Carneiro et al., 2010; Long et al., 2012; Luboshitzky et al., 2002). According to the findings of our study, asthmatic model rat erection frequency decreased, IL-6 and TNF protein expression increased, and eNOS protein expression decreased. IL-6 and TNF protein expression decreased, eNOS protein expression increased, and the number of

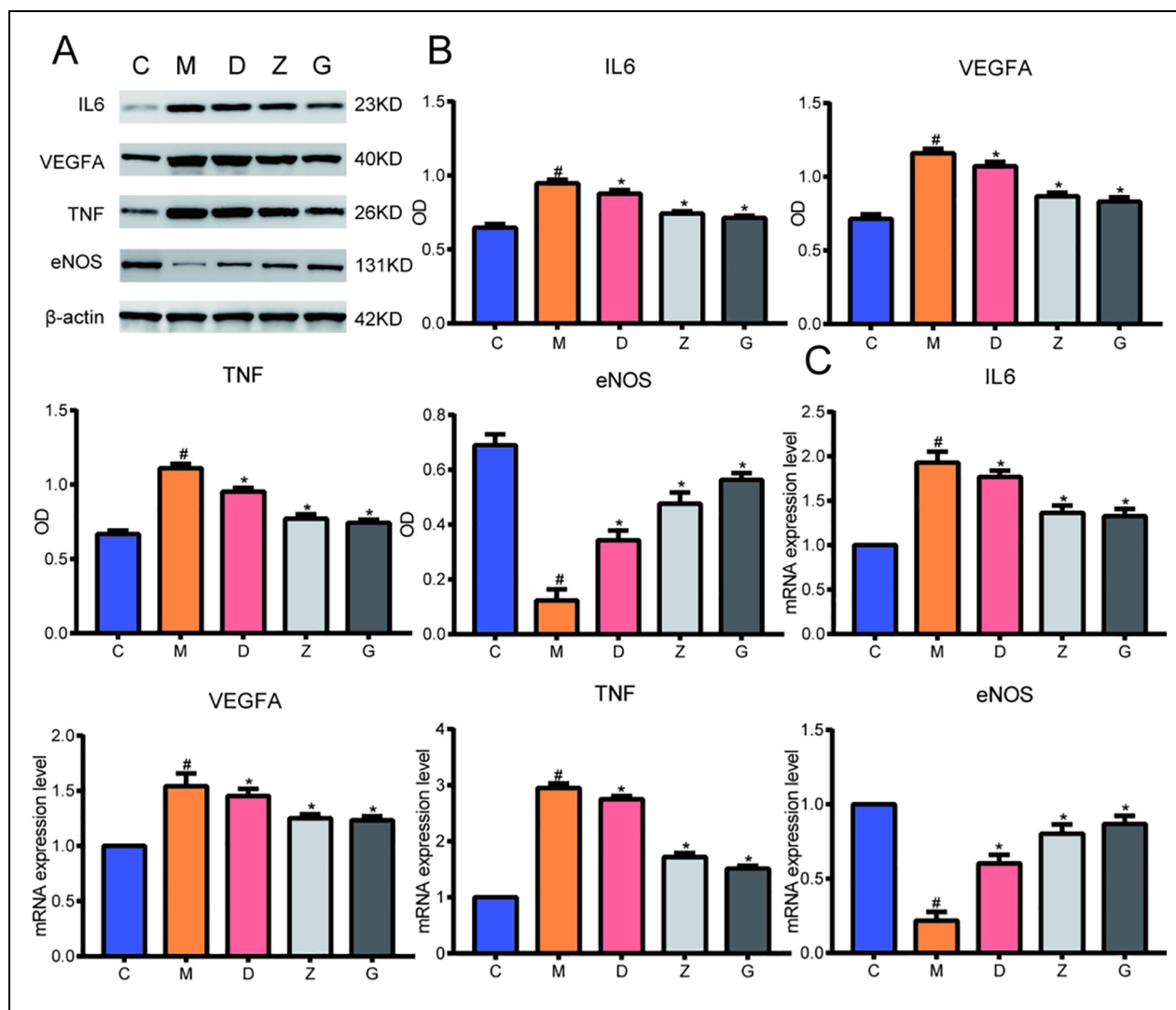


Figure 7. (A) Electrophoretogram of Three Proteins (IL6, VEGFA, TNF, eNOS) in Rats From the C, M, D, Z, and G Groups. (B) The Expression Levels of Three Proteins (IL6, VEGFA, TNF, eNOS) in Rats From the C, M, D, Z, and G Groups Determined Using Western Blotting. (C) The mRNA Expression Levels of Three Proteins (IL6, VEGFA, TNF, eNOS) in Rats From the C, M, D, Z, and G Groups Determined Using Western Blotting.

Note. Data are expressed as the mean \pm SEM. Differences with $p < .05$ were considered statistically significant.

[#] $p < .05$, the M group versus the C group; ^{*} $p < .05$, the D, Z, and G groups versus the M group.

erections increased after treatment with XFZYD. One of the mechanisms underlying the deterioration of erectile function is the increase in inflammatory factors brought on by asthma, which results in penile cavernous ischemia and hypoxia. XFZYD can improve the erectile function of asthmatic rats by lowering the expression of IL-6 and TNF protein and increasing the expression of eNOS protein.

The glycosylated peptides VEGF-A, VEGF-B, VEGF-C, VEGF-E, and placental growth factors are members of the VEGF family (X. Zhao, Yu et al., 2018). VEGF is highly expressed in tissues rich in

blood vessels, such as the trachea and the lung (H. Y. Lu et al., 2016). Inflammatory cells like neutrophils, lymphocytes, monocytes, and eosinophils also produce VEGF. VEGF induces airway remodeling by causing structural changes to the vascular extracellular matrix and interstitial edema in asthma (X. Zhao, Yu et al., 2018). VEGFA overexpression worsens by increasing vascular permeability and inflammation (Urios et al., 2019). In the present study, the asthma model group had upregulated VEGFA protein expression, reversed by XFZYD treatment. This proves that one of the mechanisms of decreased erectile function

in patients with asthma is vascular remodeling induced by VEGFA.

Damage caused by an increase in ROS such as superoxide radicals, hydrogen peroxide, and hydroxyl radicals that cause the body's oxidation levels to exceed its antioxidant defenses is known as oxidative stress (Dua et al., 2019). The balance between ROS and antioxidants is a state of imbalance. ROS functions as a signal molecule to regulate physiological processes under normal conditions. The overproduction of ROS will exacerbate the severity of patients with bronchial asthma by causing lipid peroxidation, modified protein, oxidative DNA damage, and damage to multiple organelles, impairing their function. Huang found that in the smoking-induced ED rat model, the level of ROS in rat penile tissue was significantly elevated, resulting in enhanced penile tissue apoptosis. In addition, the integrity of the penile endothelium was damaged, resulting in endothelial dysfunction and, ultimately, the occurrence of ED (Y. C. Huang et al., 2015). According to our study, the asthma model group's level of ROS significantly increased, and the smooth muscle cells in penile tissue decreased. It demonstrated that XFZYD enhances the erectile function of rats through specific antioxidant stress when the level of ROS significantly reduced, and the number of erections increases after the intervention of XFZYD.

Conclusions

We discovered that XFZYD improved erectile function in rats with asthma-associated ED while lowering IL-6, VEGFA, TNF, and ROS expression levels in penile tissue and increasing the expression level of eNOS. The above results suggest that XFZYD may improve erectile function in asthma model rats by inhibiting inflammation and reducing vascular permeability. Although further studies are necessary to elucidate the precise mechanism, this article systematically explored the possible targets associated with XFZYD to improve asthma-induced ED, which provides the theoretical basis and experimental data for future pharmacological studies. More importantly, this study provides new research ideas for interdisciplinary research on TCM treatment, which is worth promoting and learning.

Acknowledgments

All the authors of the manuscript are immensely grateful to the foundations for their valuable support.



Declaration of Conflicting Interests

The author(s) declared no potential conflicts of interest with respect to the research, authorship, and/or publication of this article.

Funding

The author(s) disclosed receipt of the following financial support for the research, authorship, and/or publication of this article: This research was supported by the National Natural Science Foundation of China (grant no. 81704086), the Talent Training Programme Project, and the Clinical Research Operating Expenses of Centralised High-Level Chinese Medicine Hospitals, and Beijing University of Chinese Medicine 2024 New Teacher Project (2024-JYB-XJSJJ-041).

ORCID iDs

Junlong Feng  <https://orcid.org/0000-0001-6836-9793>
Jisheng Wang  <https://orcid.org/0000-0002-3332-076X>

Data Availability Statement

The data that support the findings of this study are available from the corresponding author upon reasonable request.

References

- Araña Rosáinz Mde, J., Ojeda, M. O., Acosta, J. R., Elías-Calles, L. C., González, N. O., Herrera, O. T., García Álvarez, C. T., Rodríguez, E. M., Báez, M. E., Seijas, E. Á., & Valdés, R. F. (2011). Imbalanced low-grade inflammation and endothelial activation in patients with type 2 diabetes mellitus and erectile dysfunction. *The Journal of Sexual Medicine*, 8(7), 2017–2030. <https://doi.org/10.1111/j.1743-6109.2011.02277.x>
- Arifin, W. N., & Zahiruddin, W. M. (2017). Sample size calculation in animal studies using resource equation approach. *The Malaysian Journal of Medical Sciences: MJMS*, 24(5), 101–105. <https://doi.org/10.21315/mjms2017.24.5.11>
- Broide, D., Schwarze, J., Tighe, H., Gifford, T., Nguyen, M. D., Malek, S., Van Uden, J., Martin-Orozco, E., Gelfand, E. W., & Raz, E. (1998). Immunostimulatory DNA sequences inhibit IL-5, eosinophilic inflammation, and airway hyperresponsiveness in mice. *Journal of Immunology*, 161(12), 7054–7062.
- Burnett, A. L., Nehra, A., Breau, R. H., Culkin, D. J., Faraday, M. M., Hakim, L. S., Heidelbaugh, J., Khera, M., McVary, K. T., Miner, M. M., Nelson, C. J., Sadeghi-Nejad, H., Seftel, A. D., & Shindel, A. W. (2018). Erectile dysfunction: AUA guideline. *The Journal of Urology*, 200(3), 633–641. <https://doi.org/10.1016/j.juro.2018.05.004>
- Carneiro, F. S., Webb, R. C., & Tostes, R. C. (2010). Emerging role for TNF- α in erectile dysfunction. *The Journal*

- of *Sexual Medicine*, 7(12), 3823–3834. <https://doi.org/10.1111/j.1743-6109.2010.01762.x>
- Cazzola, M., & Polosa, R. (2006). Anti-TNF-alpha and Th1 cytokine-directed therapies for the treatment of asthma. *Current Opinion in Allergy and Clinical Immunology*, 6(1), 43–50. <https://doi.org/10.1097/01.all.0000199798.10047.74>
- Chen, J. S., & Gao, Z. Y. (2017). Examples of clinical application of Xuefu Zhuyu decoction. *Modern Distance Education Chinese Traditional Medicine*, 15, 135–136.
- Chen, L., Staubli, S. E., Schneider, M. P., Kessels, A. G., Ivic, S., Bachmann, L. M., & Kessler, T. M. (2015). Phosphodiesterase 5 inhibitors for the treatment of erectile dysfunction: A trade-off network meta-analysis. *European Urology*, 68(4), 674–680. <https://doi.org/10.1016/j.eururo.2015.03.031>
- Chen, W., Gong, L., Guo, Z., Wang, W., Zhang, H., Liu, X., Yu, S., Xiong, L., & Luo, J. (2013). A novel integrated method for large-scale detection, identification, and quantification of widely targeted metabolites: Application in the study of rice metabolomics. *Molecular Plant*, 6(6), 1769–1780. <https://doi.org/10.1093/mp/sss080>
- Chou, K. T., Huang, C. C., Chen, Y. M., Perng, D. W., Chao, H. S., Chan, W. L., & Leu, H. B. (2011). Asthma and risk of erectile dysfunction – A nationwide population-based study. *The Journal of Sexual Medicine*, 8(6), 1754–1760. <https://doi.org/10.1111/j.1743-6109.2011.02242.x>
- Diouf, I., Fievet, N., Doucouré, S., Ngom, M., Andrieu, M., Mathieu, J. F., Gaye, A., Thiaw, O. T., & Deloron, P. (2007). IL-12 producing monocytes and IFN-gamma and TNF-alpha producing T-lymphocytes are increased in placentas infected by Plasmodium falciparum. *Journal of Reproductive Immunology*, 74(1–2), 152–162.
- Dorsey, P., Keel, C., Klavens, M., & Hellstrom, W. J. (2010). Phosphodiesterase type 5 (PDE5) inhibitors for the treatment of erectile dysfunction. *Expert Opinion on Pharmacotherapy*, 1(7), 1109–1122. <https://doi.org/10.1517/14656561003698131>
- Dua, K., Malya, V., Singhvi, G., Wadhwa, R., Krishna, R. V., Shukla, S. D., Shastri, M. D., Chellappan, D. K., Maurya, P. K., Satija, S., Mehta, M., Gulati, M., Hansbro, N., Collet, T., Awasthi, R., Gupta, G., Hsu, A., & Hansbro, P. M. (2019). Increasing complexity and interactions of oxidative stress in chronic respiratory diseases: An emerging need for novel drug delivery systems. *Chemico-Biological Interactions*, 299, 168–178. <https://doi.org/10.1016/j.cbi.2018.12.009>
- Garcia, A., & Barbas, C. (2011). Gas chromatography-mass spectrometry (GC-MS)-based metabolomics. *Methods in Molecular Biology*, 708, 191–204. https://doi.org/10.1007/978-1-61737-985-7_11
- Grigoryan, V. A., Gazimiev, M. A., Demidko, Y. L., & Baidualiev, A. M. (2018). Dosage forms of sildenafil in the management of erectile dysfunction. *Urologiia*, 2018(1), 159–162.
- Hamosh, A., Scott, A. F., Amberger, J. S., Bocchini, C. A., & McKusick, V. A. (2005). Online Mendelian Inheritance in Man (OMIM), a knowledgebase of human genes and genetic disorders. *Nucleic Acids Research*, 33, D514–D517. <https://doi.org/10.1093/nar/gki033>
- Han, Z. H. (2020). Pharmacological analysis of Xuefu Zhuyu decoction and examples of proven cases. *Inner Mongolia Traditional Chinese Medicine*, 39, 69–71.
- Huang, Y. C., Chin, C. C., Chen, C. S., Shindel, A. W., Ho, D. R., Lin, C. S., & Shi, C. S. (2015). Chronic cigarette smoking impairs erectile function through increased oxidative stress and apoptosis, decreased nNOS, endothelial and smooth muscle contents in a rat model. *PLOS ONE*, 10(10), Article e0140728. <https://doi.org/10.1371/journal.pone.0140728>
- Huang, Y. T., van der Hoorn, D., Ledahawsky, L. M., Motyl, A. A. L., Jordan, C. Y., Gillingwater, T. H., & Groen, E. J. N. (2019). Robust comparison of protein levels across tissues and throughout development using standardized quantitative western blotting. *Journal of Visualized Experiments: JoVE*, 182(146), 10379159438. <https://doi.org/10.3791/59438>
- Jia, R. B., Shao, Y. F., Jiang, W. X., Chen, J. M., Zheng, J. W., Su, S. Z., & Wang, Y. L. (2020). Effect of antidepressant Puyu capsule on sexual function of male rats and its mechanism. *Chinese Pharmacology Bull*, 36, 282–288.
- Li, S., Liu, S. P., Wu, Y., Liang, L. J., Xie, Z. H., & Shi, Z. C. (2022). Shi Zhichao's experience in the treatment of difficult diseases with blood mansions and blood stasis tang. *Jilin Traditional Chinese Medicine*, 42, 900–902.
- Lin, S. H., Huang, H. B., & Lin, X. Q. (2018). Effect of modified Xuefu Zhuyu decoction on 60 cases of impotence. *Chinese Foreign Medicine Journal*, 37, 173–175.
- Long, T., Liu, G., Wang, Y., Chen, Y., Zhang, Y., & Qin, D. (2012). TNF- α , erectile dysfunction, and NADPH oxidase-mediated ROS generation in corpus cavernosum in high-fat diet/streptozotocin-induced diabetic rats. *The Journal of Sexual Medicine*, 9(7), 1801–1814. <https://doi.org/10.1111/j.1743-6109.2012.02739.x>
- Lu, C. C. (2012). Asthma and risk of erectile dysfunction in Taiwan – Patient-based or population-based? *The Journal of Sexual Medicine*, 9(3), 943. <https://doi.org/10.1111/j.1743-6109.2011.02575.x>
- Lu, H. Y., Zhao, G. L., & Fu, M. F. (2016). Polymorphisms in the vascular endothelial growth factor (VEGF) gene associated with asthma. *Genetics and Molecular Research: GMR*, 15(2), 10.4238/gmr.15027880. <https://doi.org/10.4238/gmr.15027880>
- Luboshitzky, R., Aviv, A., Hefetz, A., Herer, P., Shen-Orr, Z., Lavie, L., & Lavie, P. (2002). Decreased pituitary-gonadal secretion in men with obstructive sleep apnea. *The Journal of Clinical Endocrinology and Metabolism*, 87(7), 3394–3398. <https://doi.org/10.1210/jcem.87.7.8663>
- Ma, T. T., Zhang, G. L., Dai, C. F., Zhang, B. R., Cao, K. X., Wang, C. G., Yang, G. W., & Wang, X. M. (2020). Scutellaria barbata and Hedyotis diffusa herb pair for breast cancer treatment: Potential mechanism based on

- network pharmacology. *Journal of Ethnopharmacology*, 259, 112929. <https://doi.org/10.1016/j.jep.2020.112929>
- Musicki, B., & Burnett, A. L. (2006). eNOS function and dysfunction in the penis. *Experimental Biology and Medicine*, 231(2), 154–165. <https://doi.org/10.1177/153537020623100205>
- Papi, A., Brightling, C., Pedersen, S. E., & Reddel, H. K. (2018). Asthma. *The Lancet*, 391(10122), 783–800. [https://doi.org/10.1016/S0140-6736\(17\)33311-1](https://doi.org/10.1016/S0140-6736(17)33311-1)
- Park, J., Chai, J. S., Kim, S. W., Paick, J. S., & Cho, M. C. (2018). Inhibition of Jun N-terminal kinase improves erectile function by alleviation of cavernosal apoptosis in a rat model of cavernous nerve injury. *Urology*, 113, 253.e9–253.e16. <https://doi.org/10.1016/j.urology.2017.11.040>
- Proboszcz, M., Papińska-Goryca, M., Nejman-Gryz, P., Górska, K., & Krenke, R. (2017). A comparative study of sTREM-1, IL-6 and IL-13 concentration in bronchoalveolar lavage fluid in asthma and COPD: A preliminary study. *Advances in Clinical and Experimental Medicine: Official Organ Wrocław Medical University*, 26(2), 231–236.
- Rappaport, N., Fishilevich, S., Nudel, R., Twik, M., Belinky, F., Plaschkes, I., Stein, T. I., Cohen, D., Oz-Levi, D., Safran, M., & Lancet, D. (2017). Rational confederation of genes and diseases: NGS interpretation via GeneCards, MalaCards and VarElect. *Biomedical Engineering Online*, 16(Suppl. 1), 72. <https://doi.org/10.1186/s12938-017-0359-2>
- Siwicz, J., Zaborowski, T., Jankowska, O., Wojas-Krawczyk, K., Krawczyk, P., & Milanowski, J. (2009). Evaluation of Th1/Th2 lymphocyte balance and lipopolysaccharide receptor expression in asthma patients. *Pneumonologia I Alergologia Polska*, 7(2), 123–130.
- Szklarczyk, D., Morris, J. H., Cook, H., Kuhn, M., Wyder, S., Simonovic, M., Santos, A., Doncheva, N. T., Roth, A., Bork, P., Jensen, L. J., & von Mering, C. (2017). The STRING database in 2017: Quality-controlled protein-protein association networks, made broadly accessible. *Nucleic Acids Research*, 45(D1), D362–D368. <https://doi.org/10.1093/nar/gkw937>
- Urios, A., Ordoño, F., García-García, R., Mangas-Losada, A., Leone, P., José Gallego, J., Cabrera-Pastor, A., Megías, J., Fermin Ordoño, J., Felipe, V., & Montoliu, C. (2019). Tadalafil treatment improves inflammation, cognitive function, and mismatch negativity of patients with low urinary tract symptoms and erectile dysfunction. *Scientific Reports*, 9(1), 17119. <https://doi.org/10.1038/s41598-019-53136-y>
- Vinay, J., Moreno, D., Rajmil, O., Ruiz-Castañe, E., & Sanchez-Curbelo, J. (2021). Penile low intensity shock wave treatment for PDE5I refractory erectile dysfunction: A randomized double-blind sham-controlled clinical trial. *World Journal of Urology*, 39(6), 2217–2222. <https://doi.org/10.1007/s00345-020-03373-y>
- Vlachopoulos, C., Aznaouridis, K., Ioakeimidis, N., Rokkas, K., Vasiliadou, C., Alexopoulos, N., Stefanadi, E., Askitis, A., & Stefanadis, C. (2006). Unfavourable endothelial and inflammatory state in erectile dysfunction patients with or without coronary artery disease. *European Heart Journal*, 27(22), 2640–2648. <https://doi.org/10.1093/eurheartj/ehl341>
- Vos, T., Flaxman, A. D., Naghavi, M., Lozano, R., Michaud, C., Ezzati, M., Shibuya, K., Salomon, J. A., Abdalla, S., Aboyans, V., Abraham, J., Ackerman, I., Aggarwal, R., Ahn, S. Y., Ali, M. K., Alvarado, M., Anderson, H. R., Anderson, L. M., Andrews, K. G., & Memish, Z. A. (2012). Years lived with disability (YLDs) for 1160 sequelae of 289 diseases and injuries 1990–2010: A systematic analysis for the Global Burden of Disease Study 2010. *The Lancet*, 380(9859), 2163–2196. [https://doi.org/10.1016/S0140-6736\(12\)61729-2](https://doi.org/10.1016/S0140-6736(12)61729-2)
- Wang, J. S., Gong, X., Deng, S., Meng, F., Dai, H., Bao, B., Feng, J., Li, H., & Wang, B. (2020). Effect of asthma on erectile dysfunction in rats as determined by biological network analysis. *Medical Science Monitor: International Medical Journal of Experimental and Clinical Research*, 26, e927491. <https://doi.org/10.12659/MSM.927491>
- Wang, J. S., Feng, J. L., Li, X., Chen, Z. L., Bao, B. H., Deng, S., Dai, H. H., Meng, F. C., Wang, B., & Li, H. S. (2021). Effect of leech-centipede medicine on improving erectile function in diabetes-induced erectile dysfunction rats via PDE5 signalling pathway-related molecules. *Pharmaceutical Biology*, 59(1), 167–174. <https://doi.org/10.1080/13880209.2021.1878237>
- Wang, J. S., Li, X., Chen, Z. L., Feng, J. L., Bao, B. H., Deng, S., Dai, H. H., Meng, F. C., Wang, B., & Li, H. S. (2021). Effect of leech-centipede medicine on improving erectile function in DIED rats via PKC signalling pathway-related molecules. *Journal of Ethnopharmacology*, 267, 113463. <https://doi.org/10.1016/j.jep.2020.113463>
- Wang, Z. R., Wang, Q., Sui, Y., Zhang, Z. L., Jia, F. J., Fan, J., & Zhang, Z. J. (2018). Dexamethasone alleviates allergic asthma immature rat through toll like receptor 4. *European Review for Medical and Pharmacological Sciences*, 2(1), 184–189. https://doi.org/10.26355/eurrev_201801_14116
- Wu, J. H., & Chen, X. Y. (2013). The modern pharmacological research progress of Xuefu Zhuyu decoction. *Chinese Medicine*, 35, 1054–1058.
- Wu, Z. D., Pan, C. X., & Qin, L. Y. (2000). Observation on 61 cases of bronchial asthma treated with Xuefu Zhuyu decoction. *Henan Traditional Chinese Medicine*, 20(06), 43.
- Xiong, Y., Hu, S., Zhou, H., Zeng, H., He, X., Huang, D., & Li, X. (2019). High-throughput 16S rDNA sequencing of the pulmonary microbiome of rats with allergic asthma. *Genes & Diseases*, 7(2), 272–282. <https://doi.org/10.1016/j.gendis.2019.03.006>
- Zhang, X. C. (1977). *Ginseng and Xi Lu in medicine*. Hebei People's Publishing House.
- Zhao, F., Zhao, Q., Zhao, K. C., & Zhao, Y. (2018). Research on the progress of Chinese medicine treatment for erectile dysfunction. *China Continuing Medicine Education*, 10(32), 131–133.

- Zhao, R. L., & He, Y. M. (2018). Network pharmacology analysis of the anti-cancer pharmacological mechanisms of *Ganoderma lucidum* extract with experimental support using Hepa1-6-bearing C57 BL/6 mice. *Journal of Ethnopharmacology*, *210*, 287–295. <https://doi.org/10.1016/j.jep.2017.08.041>
- Zhao, X., Yu, F. Q., Huang, X. J., Xu, B. Y., Li, Y. L., Zhao, X. Y., Guo, H. F., & Luan, B. (2018). Azithromycin influences airway remodeling in asthma via the PI3K/Akt/MTOR/HIF-1 α /VEGF pathway. *Journal of Biological Regulators and Homeostatic Agents*, *32*(5), 1079–1088.
- Zimmerman, J. J. (2002). Congenital heart disease, cardiopulmonary bypass, systemic inflammatory response syndrome, compensatory anti-inflammatory response syndrome, and outcome: Evolving understanding of critical care inflammation immunology. *Critical Care Medicine*, *30*(5), 1178–1179. <https://doi.org/10.1097/00003246-200205000-00048>
- Zou, Z. L., Xin, C. X., Wu, Q., Jiang, R., Han, D. J., & Zhang, Z. J. (2015). Asthma inhibits erectile function in rats. *Sichuan Medicine*, *36*, 1244–1248.